

## High-Resolution X-ray Structure of an Acyl-Enzyme Species for the Class D OXA-10 $\beta$ -Lactamase

Laurent Maveyraud,<sup>†</sup> Dasantila Golemi-Kotra,<sup>‡</sup> Akihiro Ishiwata,<sup>‡</sup>  
Oussama Meroueh,<sup>‡</sup> Shahriar Mobashery,<sup>\*,‡</sup> and Jean-Pierre Samama<sup>\*,†</sup>

Contribution from Groupe de Cristallographie Biologique, Institut de Pharmacologie et de Biologie Structurale du CNRS, 205 route de Narbonne, 31077-Toulouse Cedex, France, and Institute for Drug Design and the Department of Chemistry, Wayne State University, Detroit, Michigan 48202-3489

Received July 31, 2001

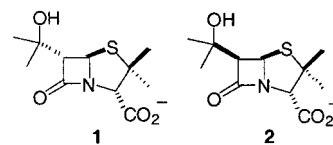
**Abstract:**  $\beta$ -Lactamases are resistance enzymes for  $\beta$ -lactam antibiotics. These enzymes hydrolyze the  $\beta$ -lactam moieties of these antibiotics, rendering them inactive. Of the four classes of known  $\beta$ -lactamases, the enzymes of class D are the least understood. We report herein the high-resolution (1.9 Å) crystal structure of the class D OXA-10  $\beta$ -lactamase inhibited by a penicillanate derivative. The structure provides evidence that the carboxylated Lys-70 (a carbamate) is intimately involved in the mechanism of the enzyme.

$\beta$ -Lactamases are bacterial resistance enzymes for  $\beta$ -lactam antibiotics.<sup>1,2</sup> Four classes of  $\beta$ -lactamases (classes A, B, C, and D) are known, each of which appears to catalyze the same reaction by a distinct mechanism.<sup>3</sup> Class D  $\beta$ -lactamases are the least understood, despite the fact that currently 37 of these enzymes have been identified.

The first X-ray structures of a class D (OXA-10)  $\beta$ -lactamase became available recently.<sup>4–6</sup> Only recently it has become evident that this enzyme has an uncommon lysine carbamate (“carboxylated” lysine, the product of the reaction of carbon dioxide and the lysine side chain amine) in its active site, a residue critical for the function of the enzyme.<sup>6</sup> The X-ray structure suggests that this carboxylated lysine should be the residue that promotes acylation of the active site serine by the substrate and also activates the hydrolytic water molecule for the deacylation step of the acyl-enzyme species. Carboxylated lysine is seen in a handful of other proteins such as rubisco,<sup>7</sup> urease,<sup>8</sup> phosphotriesterase,<sup>9</sup> dihydroorotase,<sup>10</sup> and alanine racemase.<sup>11</sup> In these enzymes the carboxylated lysine is typically

involved as a ligand for a metal ion or serves as a structural role in the enzyme. In the case of rubisco, the carbamate is coordinated to the metal ion and is proposed as an active-site base.<sup>12</sup> In this report we present structural evidence for a class D enzyme (OXA-10) inhibited by a substrate analogue that documents the involvement of carboxylated lysine in the catalytic process, a feature that sets this enzyme apart from all other  $\beta$ -lactamases.

We have described the use of 6-hydroxyalkylpenicillanates as probes for mechanisms of  $\beta$ -lactamases.<sup>13</sup> These molecules are useful in delineating the direction of approach of the hydrolytic water to the acyl-enzyme species. In general, if the water molecule approaches the acyl-enzyme species from the  $\alpha$  direction,  $\alpha$ -hydroxyalkylpenicillanates inhibit the enzymes, as is the case with class A  $\beta$ -lactamases. The opposite is true for class C  $\beta$ -lactamases, for which  $\beta$ -hydroxyalkylpenicillanates are inhibitors. However, we noted that both  $\alpha$ - and  $\beta$ -hydroxyisopropylpenicillanates (**1** and **2**) were irreversible inhibitors for the class D OXA-10  $\beta$ -lactamase. The kinetics of  $\beta$ -lactamase



inhibition were analyzed by Kitz and Wilson plots<sup>14</sup> to evaluate the first-order rate constant ( $k_{inact}$ ) for inhibition and the  $K_I$  values, which are akin to  $K_m$  for enzyme substrates. Compounds **1** and **2** inactivated the enzyme with the first-order rate constants

- <sup>†</sup> Institut de Pharmacologie et de Biologie Structurale du CNRS.  
<sup>‡</sup> Wayne State University.
- (1) Bush, K.; Mobashery, S. *Adv. Exp. Med. Biol.* **1998**, 456, 71.
  - (2) Bush, K. *Clin. Infect. Dis.* **2001**, 32, 1085.
  - (3) Kotra, L. P.; Samama, J. P.; Mobashery, S. In *Bacterial Resistance to Antimicrobials, Mechanisms, Genetics, Medical Practice and Public Health*; Lewis, A., Salyers, Haber, H., Wax, R. G., Eds.; Marcel Dekker: New York, 2001; p 123.
  - (4) (a) Golemi, D.; Maveyraud, L.; Vakulenko, S.; Tranier, S.; Ishiwata, A.; Kotra, L. P.; Samama, J. P.; Mobashery, S. *J. Am. Chem. Soc.* **2000**, 122, 6132. (b) Golemi, D.; Maveyraud, L.; Vakulenko, S.; Samama, J. P.; Mobashery, S. *Proc. Acad. Sci. U.S.A.* **2001**, 98, 14280–14285.
  - (5) Paetzel, M.; Danel, F.; de Castro, L.; Mosimann, S. C.; Page, M. G.; Strynadka, N. C. *Nat. Struct. Biol.* **2000**, 7, 918.
  - (6) Maveyraud, L.; Golemi, D.; Kotra, L. P.; Tranier, S.; Vakulenko, S.; Mobashery, S.; Samama, J. P. *Structure* **2000**, 8, 1289.
  - (7) Lorimer, G. H.; Badger, M. R.; Andrews, T. J. *Biochemistry* **1976**, 15, 529.
  - (8) Jabri, E.; Carr, M. B.; Hausinger, R. P.; Karplus, P. A. *Science* **1995**, 268, 998.
  - (9) Shim, H.; Raushel, F. M. *Biochemistry* **2000**, 39, 7357.
  - (10) Thoden, J. B.; Philips, G. N.; Neal, T. M.; Raushel, F. M.; Holden, H. M. *Biochemistry* **2001**, 40, 6989.

- (11) Morollo, A. A.; Petsko, G. A.; Ringe, D. *Biochemistry* **1999**, 38, 3293.
- (12) Cleland, W. W.; Andrews, T. J.; Gutteridge, S.; Hartman, F. C.; Lorimer, G. H. *Chem. Rev.* **1998**, 98, 549.
- (13) Golemi, D.; Maveyraud, L.; Ishiwata, A.; Tranier, S.; Miyashita, K.; Nagase, T.; Massova, I.; Mourey, L.; Samama, J. P.; Mobashery, S. *J. Antibiot.* **2000**, 53, 1022 and the references therein.
- (14) Kitz, R.; Wilson, I. B. *J. Biol. Chem.* **1962**, 237, 3245.

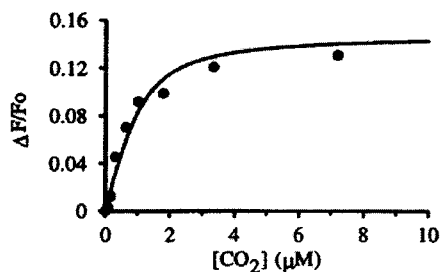


**Figure 1.** Relative change of the intrinsic tryptophan fluorescence of the OXA-10  $\beta$ -lactamase vs total carbon dioxide concentration described by equation in Experimental Procedures.

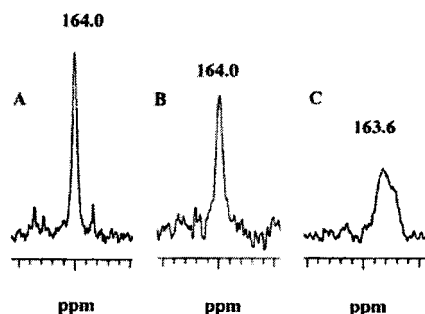


**Figure 2.**  $^{13}\text{C}$  NMR spectra in the region for the carbamate signal for the native OXA-10  $\beta$ -lactamase (A), enzyme inhibited by **1** (B), and enzyme inhibited by **2** (C). Enzyme concentration was 1.0 mM in each case.

( $k_{\text{inact}}$ ) of  $(1.3 \pm 0.1) \times 10^{-4}$  and  $(5.2 \pm 0.1) \times 10^{-4} \text{ s}^{-1}$ , respectively. The  $K_{\text{I}}$  values for the two inhibitors were  $300 \pm 100$  and  $240 \pm 10 \mu\text{M}$ , respectively. So the kinetics of enzyme inhibition with both compounds were comparable. This was an unexpected finding, for which we attempted to provide the structural explanations by analyses of the  $^{13}\text{C}$  NMR spectra and the X-ray structure for the inhibited complexes.

The OXA-10 enzyme binds carbon dioxide reversibly (to produce the carbamate). The data from the fluorescence experiments were plotted as quenching of the intrinsic tryptophan fluorescence vs the total carbon dioxide concentration (Figure 1). The  $K_{\text{d}}$  for carbon dioxide binding to the enzyme was  $0.3 \pm 0.1 \mu\text{M}$ . Figure 1 indicates that addition of carbon dioxide to the enzyme resulted in a saturable and concentration-dependent quenching of tryptophan fluorescence.

We were able to decarboxylate the carbamate of the enzyme by briefly incubating it at pH 4.5, which resulted in an enzyme that lacked activity. The pH of the protein solution was adjusted to 7.5, and  $^{13}\text{C}$ -labeled sodium bicarbonate was added to the mixture. The  $^{13}\text{C}$  NMR spectrum of the native protein (Figure 2A) showed the carbamate signal at 164 ppm. The same chemical shift for a carboxylated lysine in rubisco<sup>15</sup> and phosphotriesterase<sup>16</sup> has been reported. This signal was only broadened slightly, when the enzyme was inhibited by **1** (Figure 2B), whereas it was broadened significantly and shifted upfield in the complex with **2** (Figure 2C). These results indicate that the enzyme in complex with **2** has strong electrostatic interactions between the carbamate and the inhibitor and only weak electrostatic interactions or none in the complex with **1**.

Repeated attempts at obtaining a crystal for the complex of the OXA-10 enzyme with **1** were unsuccessful, in contrast to

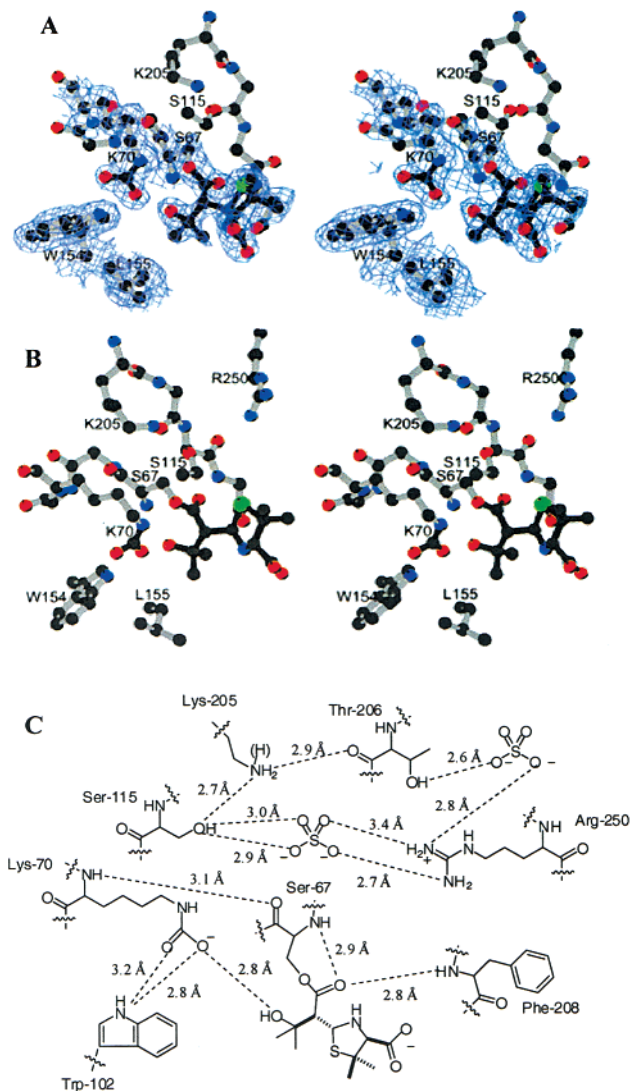


**Figure 3.** (A) Initial  $2F_{\text{obs}} - F_{\text{calc}}$  electron density map contoured at one standard deviation above the mean. The final refined model of the OXA-10  $\beta$ -lactamase inhibited by **2** (at 1.9 Å resolution) is superimposed. The carbamate function on Lys-70 and inhibitor **2** are displayed with black bonds. (B) A different view of the structure without the electron density. (C) A schematic for the interactions of the inhibitor in the active site. The distances are for the separation between heteroatoms.

the case of inhibitor **2**. Crystals were soaked with compound **1** at various concentrations between 6 and 15 min. At short soaking times, there was no substitution in the active site, whereas longer soaking times led to disruption of the crystal lattice. The soaking time at which diffraction was lost with compound **1** corresponded to the minimum soaking time required for full binding of compound **2** to the enzyme. We therefore suggest that binding of compound **2** to the active site induced a conformational change of the enzyme–inhibitor complex. Cocrystallization was not possible by the spontaneous hydrolysis of compound **1** that occurred at pH 8.5 during the 2 weeks required for crystal growth.

The crystal structure of the OXA-10  $\beta$ -lactamase inhibited by **2** showed that each subunit of the two dimers in the asymmetric unit was acylated at the catalytic Ser-67. In addition, as already observed in the native protein structure,<sup>6</sup> Lys-70 was carboxylated in all subunits (Figure 3A). In the acylated complex, the oxygen atom of the carbonyl of the ester group is

(15) O'Leary, M. H.; Jaworski, R. J.; Hartman, F. C. *Proc. Natl. Acad. Sci. U.S.A.* **1979**, *76*, 673.

(16) Hong, S.-B.; Kuo, J. M.; Mullins, L. S.; Raushel, F. M. *J. Am. Chem. Soc.* **1995**, *117*, 7580.

ensconced in the oxyanion hole, at hydrogen bond distance to the backbone nitrogen atoms of Ser-67 (3.0 Å) and Phe-208 (2.9 Å). A similar interaction is found in most structures of acyl-enzyme complexes of class A or class C of  $\beta$ -lactamases. However, binding of **2** to the OXA-10 enzyme displayed a striking and unique difference when compared to the related complexes with other serine  $\beta$ -lactamases; the carboxylate group at C<sub>3</sub> of the thiazolidine ring does not lie along the  $\beta$ -strand S3 toward Lys-205 and Arg-250 but points outside the active site. These residues, which are structurally equivalent to Lys-234 and Arg-244 in class A enzymes, are more than 10 Å away from the carboxylate group. In this conformation, the two methyl groups at C<sub>2</sub> of **2** are located in the hydrophobic environment provided by the side chains of Met-99, Trp-102, and Phe-208.

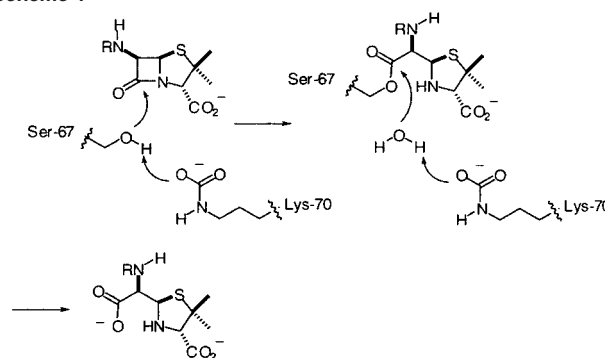
Binding of **2** to the OXA-10  $\beta$ -lactamase contrasts to the cases of the acyl-enzyme structures of class A enzymes, in which Lys-234 and Arg-244 serve as anchors for the C<sub>3</sub> carboxylate groups of substrates and inhibitors. Such a canonical conformation seems to be impaired in the case of OXA-10 acylated by **2**, by a steric conflict between the 6 $\beta$ -hydroxyisopropyl moiety and the main-chain atoms of residue 208. This conflict is alleviated with the smaller 6 $\beta$  substitutes found in typical substrates for which canonical binding is possible. The carboxylate group at C<sub>3</sub> of the thiazolidine ring would be located where a sulfate ion binds in the native OXA-10 enzyme, at hydrogen bond distance to Arg-250.

In the X-ray structure (parts A and B of Figure 3), the hydroxyl group of the 6 $\beta$ -hydroxyisopropyl substituent is at hydrogen bonding distance to the main-chain nitrogen atom of Ser-67 (2.9 Å) and to one oxygen of the carbamate group of Lys-70 (2.7 Å), as it was anticipated from the <sup>13</sup>C NMR experiment (Figure 2C). In the crystallographic structures of the class A TEM-1<sup>17</sup> and NMCA<sup>18</sup>  $\beta$ -lactamases inhibited by hydroxyalkylpenicillanates, the hydroxyl groups interact with the hydrolytic water molecule bound to Glu-166. Comparison of these structures with the OXA-10  $\beta$ -lactamase acylated by **2** revealed that one oxygen atom of the carbamate group occupies a position similar to that of a carboxylate oxygen atom of Glu-166 of class A enzymes.

In addition, the hydroxyl group of the 6 $\beta$ -hydroxyisopropyl moiety in the OXA-10 inhibited complex superimposes the position of the hydrolytic water molecule in the acyl-enzyme species of the class A enzymes. We state here that the hydroxyl moiety of **2** bound to the OXA-10 enzyme (parts A and B of Figure 3) occupies the position of the deacylating water molecule. A schematic presentation is provided in Figure 3C. In this arrangement, this water molecule would be activated by the carbamate group of Lys-70 (2.7 Å) and would be ideally placed for hydrolysis of the acyl-enzyme intermediate. Compound **2** inhibits the enzyme irreversibly because the binding location of the hydroxyl of the inhibitor precludes the existence of the water molecule that would hydrolyze the acyl-enzyme species.

The structure of the native enzyme without any ligand bound to the active site revealed direct interaction between one oxygen of the carbamate and the side chain hydroxyl of Ser-67.<sup>6</sup> Hence, the carbamate is the only conceivable residue for activation of

Scheme 1



the side chain of serine for the acylation event. Scheme 1 summarizes our views on the mechanism of substrate turnover chemistry by the OXA-10  $\beta$ -lactamase.

In light of the crystallographic difficulties with **1**, a computational model of the acyl-enzyme species of **1** with the OXA-10 enzyme was generated. The thiazolidine carboxylate at C<sub>3</sub> is within hydrogen bonding distance of Arg-250, and analysis of a 300 ps molecular dynamics simulation showed that the ester carbonyl oxygen of the acylated species is anchored within the oxyanion hole with hydrogen bonding interactions with the backbone nitrogen atoms of Phe-208 and Ser-67 (2.8 Å each). A plot of these distances as a function of time showed small fluctuations of these bonds (rarely exceeding 0.3 Å) within the simulation time frame. The hydroxyl group of the hydroxyisopropyl moiety in this acyl-enzyme species is near the carboxylated lysine, but in contrast to the X-ray structure for **2**, the possibility of hydrogen bonding is substantially less favorable. Over the period of the 300 ps trajectory, the angle for a potential hydrogen bond between the hydroxyl of the inhibitor and the carbamate group fluctuated around  $105^\circ \pm 10^\circ$ , making hydrogen bonding unfavorable, consistent with the NMR data (Figure 2B). The location of the hydroxyisopropyl group of **1** in the complex, however, prevents the travel of the hydrolytic water toward the ester moiety for steric reasons, accounting for the irreversible inhibition of the enzyme.

What has been detailed in this report underscores the fact that the selection pressure for evolution of drug resistant enzymes against  $\beta$ -lactam antibiotics has been considerable, precipitating a set of events for the advent of at least four distinct catalytic mechanisms for turnover of these antibiotics in resistant bacteria. In the case of class D enzymes, carboxylated Lys-70 is a key mechanistic player.

## Experimental Procedures

Penicillin G was purchased from Sigma. The growth medium was purchased either from Difco Laboratories (Detroit, MI) or Fisher Scientific. The chromatography media were from BioRad Laboratories, and NaH<sup>13</sup>CO<sub>3</sub> (99% enriched) was purchased from Cambridge Isotope Lab. Isolation and purification of OXA-10 enzyme were carried out as described earlier.<sup>4</sup>

**Enzyme Assay.** All kinetics measurements were performed on a Hewlett-Packard 8453 diode array spectrophotometer, at room temperature in 100 mM sodium phosphate buffer (pH 7.0). The enzyme activity was measured by monitoring the hydrolysis of penicillin G ( $\Delta\epsilon_{240} = 570 \text{ cm}^{-1} \text{ M}^{-1}$ ).

**Determination of Carbon Dioxide Binding Constant.** Carboxylates are known to quench tryptophan fluorescence in proteins.<sup>19</sup> Carboxylation of the lysine by carbon dioxide quenches the emission from Trp-

(17) Maveyraud, L.; Massova, I.; Birck, C.; Miyashita, K.; Samama, J. P.; Mobashery, S. *J. Am. Chem. Soc.* **1996**, *118*, 7435.

(18) Mourey, L.; Miyashita, K.; Swarén, P.; Bulychev, A.; Samama, J. P.; Mobashery, S. *J. Am. Chem. Soc.* **1998**, *120*, 9383.



154, an active-site residue in OXA-10. The enzyme was incubated with degassed 25 mM sodium acetate, pH 4.5 buffer, to allow decarboxylation of the carbamate (assay of activity at pH 7.0 showed roughly 10% activity remaining). The pH of the solution was adjusted to 7.5 by degassed 100 mM sodium phosphate buffer, pH 7.5. The enzyme (1  $\mu$ M) was excited at 295 nm, and emission was recorded at 340 nm. Aliquots of concentrated NaHCO<sub>3</sub>, prepared in the above buffer, were added to the enzyme solution to provide the desired carbon dioxide concentrations, as per a literature method.<sup>20</sup> The data were fitted using the Graft software for a single binding site model by the following equation:

$$\frac{\Delta F}{F_0} = \frac{\Delta F_{\max}}{2F_0[E]_t} \{a - (a^2 - 4[E]_t[L]_t)^{1/2}\}$$

where  $a = K_d + [E]_t + [L]_t$ ,  $F_0$  is the initial intrinsic fluorescence of the protein,  $\Delta F$  is the change in fluorescence,  $\Delta F_{\max}$  is the maximum change in fluorescence after saturation by carbon dioxide,  $[L]_t$  is the concentration of total carbon dioxide, and  $[E]_t$  is the enzyme concentration in the assay. The analysis of the data was done according to literature methods.<sup>21,22</sup>

#### Determination of Kinetics Parameters for Enzyme Inhibition.

Enzyme inhibition experiments were commenced by the addition of a portion of a stock solution of the inhibitor (1–3 mM final concentrations) in buffer containing 5  $\mu$ M enzyme at ice–water temperature. A 10  $\mu$ L portion of the mixture was removed at various time intervals and was mixed with 490  $\mu$ L of the assay mixture containing 0.8 mM benzylpenicillin in 100 mM sodium phosphate buffer, pH 7.0, to measure the residual enzyme activity. The activity was monitored at 240 nm until the substrate was exhausted. Data were analyzed according to the method of Kitz and Wilson.<sup>14</sup>

**<sup>13</sup>C NMR Experiments.** The OXA-10  $\beta$ -lactamase (10 mg) was incubated with degassed 25 mM sodium acetate buffer, pH 4.5, and was further subjected to dialysis against degassed 10 mM sodium phosphate buffer pH 7.5 supplemented with 0.1 mM EDTA. Subsequently, the enzyme was dialyzed against the above buffer supplemented with 20 mM <sup>13</sup>C-labeled sodium bicarbonate and then was concentrated to 1 mM. The <sup>13</sup>C NMR spectra were collected at 25 °C. The enzyme at 1 mM was incubated with 20 mM of 6 $\alpha$ -hydroxyisopropylpenicillanate or of 6 $\beta$ -hydroxyisopropylpenicillanate for 6 h or 24 h at 4 °C, and the <sup>13</sup>C NMR spectra were collected at 25 °C.

**Crystallization and Soaking.** Single crystals of the OXA-10  $\beta$ -lactamase were obtained by the hanging drop method, as previously described.<sup>6</sup> Briefly, 1  $\mu$ L of a protein solution at 10 mg/mL in 20 mM sodium potassium phosphate buffer, pH 7.8, was mixed with 1  $\mu$ L of the reservoir solution (2.0 M ammonium sulfate, 100 mM Tris-HCl, pH 8.5) at 4 °C. Crystals of average size 300  $\times$  300  $\times$  50  $\mu$ m<sup>3</sup> were obtained after 2 weeks. Protein–inhibitor complexes were prepared by a 15 min soaking of the crystal in a solution of **2** (100 mM), ammonium sulfate (2.2 M), and Tris-HCl (100 mM), pH 8.5. The crystal was then immersed for about 40 s in the cryoprotecting solution (ethylene glycol 20% (v/v), 2.2 M ammonium sulfate, 100 mM Tris-HCl, pH 8.5) before cryocooling in a stream of nitrogen gas at 100 K.

**Data Collection.** Diffraction data were collected on the ID14 EH1 beam line at ESRF (Grenoble, France) at a wavelength of 0.934 Å. The diffracted intensities were measured to a resolution of 1.9 Å on a MAR CCD detector with a crystal to detector distance of 150 mm; 180 oscillations of 1° were collected. Reflections were integrated with MOSFLM,<sup>23</sup> scaled and merged with SCALA,<sup>24</sup> and converted to

**Table 1.** Data Processing Statistics for the Entire Resolution Range and for the Highest Resolution Shell

	34.65–1.90 Å	2.00–1.90 Å
number of observations	328 797	38212
number of unique reflections	88 380	12 129
multiplicity	3.7	3.2
completeness (%)	99.0	93.4
$R_{\text{sym}}$	0.051	0.193
$I/\sigma$	14.2	4.6

amplitudes with TRUNCATE from the CCP4 suite of programs<sup>25</sup> (Table 1). Two percent of the data were randomly selected for the calculation of the free  $R$  factor.

**Model Building and Crystallographic Refinement.** Soaking of the crystals induced variations of about 5% of the cell parameters (apoenzyme  $a = 67.3$  Å,  $b = 82.4$  Å,  $c = 101.2$  Å, and  $\beta = 95.9^\circ$ ; soaked crystals  $a = 66.1$  Å,  $b = 81.5$  Å,  $c = 106.8$  Å, and  $\beta = 94.5^\circ$ ), and the molecular replacement method was applied to derive the initial phases.

The structure of one monomer, refined to 1.8 Å resolution,<sup>6</sup> was used as a model after removal of all solvent molecules and of the carbamate group on Lys-70. The orientations and the positions in the four molecules of the asymmetric unit were found using MOLREP.<sup>26</sup> The  $\sigma_A$ -weighted electron density maps computed after rigid body refinement of the molecular replacement solution showed clear electron density extending from Ser-67OG and from Lys-70NZ in all four monomers. The structure of a serine acylated by **2** was constructed and optimized using the AM1 Hamiltonian of the program MOPAC.<sup>27</sup>

Carboxylated lysines and modified serine residues were introduced in the electron density at that stage of structure determination. Further cycles of refinement were performed using the maximum likelihood method as implemented in REFMAC,<sup>28</sup> including a bulk solvent correction. The electron density maps and the models were displayed and corrected with TURBO-FRODO. In the last steps of refinement, water molecules were automatically introduced using ARP.<sup>29</sup> Anisotropic B refinement was performed in the last cycle of refinement. The final model comprised the four OXA-10 monomers, with Ser-67 acylated by **2**, 18 sulfate anions, 10 ethylene glycol moieties, and 713 water molecules. Lysine-70 was carboxylated in all four subunits. The final  $R_{\text{factor}}$  and  $R_{\text{free}}$  values were 0.127 and 0.2106, respectively, for all data between 34.65 and 1.90 Å.

#### Computational Modeling and Molecular Dynamics Simulations.

A model for compound **1** bound to the OXA-10 enzyme was constructed on the basis of the X-ray crystallographic structures for acyl-enzyme species of class A  $\beta$ -lactamases bound in the canonical manner.<sup>18</sup> The acyl-enzyme species with compound **1** was positioned in the active site of the OXA-10  $\beta$ -lactamase such that one oxygen of the ester carbonyl of the ligand formed hydrogen-bonding interactions with residues Ser-67 and Phe-208, thus anchoring it in the oxyanion hole. Manipulation of these structures was carried out using the SYBYL 6.7 package.<sup>30</sup>

The AMBER 6<sup>31</sup> package, using the “parm99” set of parameters,<sup>32</sup> was used to carry out all energy minimizations and molecular dynamics

- (19) Chen, Y.; Barkley, M. D. *Biochemistry* **1998**, *37*, 9976.  
 (20) Butter, J. N. In *Carbon Dioxide Equilibria and their Applications*; Addison-Wesley: Reading, MA, 1982.  
 (21) Olson, S. T.; Shore, J. D. *J. Biol. Chem.* **1981**, *256*, 1165.  
 (22) Bernat, B. A.; Armstrong, R. N. *Biochemistry* **2001**, *40*, 12712.  
 (23) Leslie, A. G. W. In *Proceedings of the Daresbury Study Weekend*; Heliwell, J. R., Machin, P. A., Papiz, M. Z., Eds.; Daresbury Laboratory: Daresbury, Warrington, U.K., 1987; pp 39–50.

- (24) Evans, P. R. In *Proceedings of the Daresbury Study Weekend*; Sawyer, L., Isaacs, N., Bailey, S., Eds; Daresbury Laboratory: Daresbury, Warrington, U.K., 1993; pp 114–122.  
 (25) CCP4. *Acta Crystallogr.* **1994**, *D50*, 760.  
 (26) Vagin, A. A.; Teplyakov, A. *J. Appl. Crystallogr.* **1997**, *30*, 1022.  
 (27) Stewart, J. J. P. *Quant. Chem. Prog. Exch.* **1990**, *10*, 86.  
 (28) Murshudov, G.; Vagin, A. A.; Dodson, E. J. *Acta Crystallogr.* **1997**, *D53*, 249.  
 (29) Perrakis, A.; Sixma, T. K.; Wilson, K. S.; Lamzin, V. *Acta Crystallogr.* **1997**, *D53*, 448.  
 (30) Sybyl, version 6.7: Tripos Associates, 1699 South Hanley Rd., Suite 303, St. Louis, MO 63144.  
 (31) Case, D. A.; Pearlman, D. A.; Caldwell, J. W.; Cheatham, T. E., III; Ross, W. S.; Simmerling, C. L.; Darden, T. A.; Merz, K. M.; Stanton, R. V.; Cheng, A. L.; Vincent, J. J.; Crowley, M.; Tsui, V.; Radmer, R. J.; Duan, Y.; Pitera, J.; Massova, I.; Seibel, G. L.; Singh, U. C.; Weiner, P. K.; Kollman, P. A. *AMBER 6*; University of California, San Francisco: San Francisco, CA.

simulations. Atomic charges for compound **1** and the nonstandard carboxylated lysine were determined using the RESP method.<sup>33</sup> This consisted of first optimizing the molecules at the HF/3-21G level of theory and basis set, followed by a HF/6-31G\* single-point energy calculation to determine the electrostatic potential around the molecule, which was subsequently used in the two-stage RESP fitting procedure. All *ab initio* calculations were carried out with the Gaussian 98 suite of programs.<sup>34</sup> The acyl-enzyme complex was then immersed in a TIP3P water box with initial dimensions chosen such that no atom in the acyl-enzyme species is at a distance of less than 10 Å from any face of the box. This resulted in a completely solvated complex consisting of 39 391 atoms. The particle mesh Ewald (PME) method was used to treat long-range electrostatics.<sup>35</sup> Bonds that involve hydrogen atoms were constrained with SHAKE, and a time step of 1.5 fs was used to carry out molecular dynamics simulations.<sup>36</sup>

The following protocol was used for equilibration. Cartesian restraints were applied to the acyl-enzyme species, and 5000 steps of steepest

descent energy minimization were carried out. This was followed by a 10 ps molecular dynamics run at constant pressure, where the temperature was gradually increased from 100 to 300 K in the first 1.5 ps, followed by 8.5 ps of simulations at 300 K. Subsequently, a series of six steepest descent energy minimizations, each consisting of 1000 steps, were carried out by gradually relaxing the restraints on the acyl-enzyme complex. Subsequently, the entire system was subjected to a series of three molecular dynamics runs. First, the system was gradually heated from 0 to 100 K in 1.5 ps, followed by 8.5 ps of simulation at 100 K. A similar procedure was carried out from 100 to 200 K and then from 200 to 300 K. Finally, a total of 45 ps of equilibration molecular dynamics simulation was carried out at 300 K. For all constant-temperature simulations, the Berendsen method is used to keep the temperature fixed.<sup>37</sup>

Equilibration was followed by a 300 ps production run with coordinates collected every 0.15 ps. A final model was then obtained by averaging over all structures collected during the 300 ps simulation, followed by 3000 steps of steepest descent energy minimization.

**Acknowledgment.** The work in France was funded in part by the Programme de Recherche Fondamentale en Microbiologie (MENRT) and the CNRS. The work in the U.S. was supported by a grant from the National Institutes of Health.

JA016736T

(32) Wang, J.; Cieplak, P.; Kollman, P. A. *J. Comput. Chem.* **2000**, *21*, 1049.

(33) Bayly, C. I.; Cieplak, P.; Cornell, W. D.; Kollman, P. A. *J. Chem. Phys.* **1993**, *97*, 10269.

(34) Frisch, M. J.; Trucks, G. W.; Schlegel, H. B.; Scuseria, G. E.; Robb, M. A.; Cheeseman, J. R.; Zakrzewski, V. G.; Montgomery, J. A., Jr.; Stratmann, R. E.; Burant, J. C.; Dapprich, S.; Millam, J. M.; Daniels, A. D.; Kudin, K. N.; Strain, M. C.; Farkas, O.; Tomasi, J.; Barone, V.; Cossi, M.; Cammi, R.; Mennucci, B.; Pomelli, C.; Adamo, C.; Clifford, S.; Ochterski, J.; Petersson, G. A.; Ayala, P. Y.; Cui, Q.; Morokuma, K.; Malick, D. K.; Rabuck, A. D.; Raghavachari, K.; Foresman, J. B.; Cioslowski, J.; Ortiz, J. V.; Stefanov, B. B.; Liu, G.; Liashenko, A.; Piskorz, P.; Komaromi, I.; Gomperts, R.; Martin, R. L.; Fox, D. J.; Keith, T.; Al-Laham, M. A.; Peng, C. Y.; Nanayakkara, A.; Gonzalez, C.; Challacombe, M.; Gill, P. M. W.; Johnson, B. G.; Chen, W.; Wong, M. W.; Andres, J. L.; Head-Gordon, M.; Replogle, E. S.; Pople, J. A. *Gaussian 98*; Gaussian, Inc.: Pittsburgh, PA, 1998.

(35) Darden, T. A.; M., Y. D.; Pedersen, L. G. *J. Chem. Phys.* **1993**, *98*, 10089.

(36) Ryckaer, J. P.; Ciccotti, G.; Berendsen, J. H. C. *J. Comput. Chem.* **1977**, *23*, 327.

(37) Berendsen, H. J. C.; Postma, J. P. M.; Van Gunsteren, W. F.; Dinola, A.; Haak, J. R. *J. Chem. Phys.* **1984**, *81*, 3684.